Acta Neuropathologica Communications

RESEARCH

Open Access

Partial normalization of hippocampal oscillatory activity during sleep in TgF344-AD rats coincides with increased cholinergic synapses at early-plaque stage of Alzheimer's disease

Monica van den Berg[1,5*], Loran Heymans[1,5], Daniëlle Toen[1,5], Mohit A. Adhikari[1,5], Johan Van Audekerke[1,5], Marlies Verschuuren[2,3,5], Isabel Pintelon[2,3,5], Winnok H. De Vos[2,3,5], Annemie Van der Linden[1,5], Marleen Verhoye[1,5*†] and Georgios A. Keliris[1,4,5*†]

Abstract

Sleep alterations are known to occur in Alzheimer's disease (AD), before cognitive symptoms become apparent, and are thought to play an important role in the pathophysiology of AD. However, knowledge on the extent of macro- and microstructural changes of sleep during early, presymptomatic stages of AD is limited. We hypothesize that Aβ-induced perturbations of neuronal activity disrupt this oscillatory activity during sleep at pre-plaque stages of AD. In this study, we aimed to assess hippocampal oscillatory activity during sleep at pre- and early-plaque stages of AD, by performing 24-hour hippocampal electrophysiological measurements in TgF344-AD rats and wildtype littermates at pre- and early-plaque stages of AD. To provide a mechanistic understanding, histological analysis was performed to quantify GABA-ergic, glutamatergic and cholinergic synapses. We observed a differential impact of AD on hippocampal activity during rapid eye movement (REM) and non-REM (NREM) sleep, in the absence of robust changes in circadian rhythm. TgF344-AD rats demonstrated increased duration of sharp wave-ripples during NREM sleep, irrespective of age. Interestingly, a significantly decreased theta-gamma coupling was observed in TgF344-AD rats, prior to amyloid plaque deposition, which was partially restored at the early-plaque stage. The partial recovery of hippocampal activity during REM sleep coincided with an increased number of cholinergic synapses in the hippocampus during the early-plaque stage in TgF344-AD rats, suggestive of basal

†Marleen Verhoye and Georgios A. Keliris contributed equally to this work.

*Correspondence:
Monica van den Berg
monica.vandenberg@uantwerpen.be
Marleen Verhoye
marleen.verhoye@uantwerpen.be
Georgios A. Keliris
georgios.keliris@outlook.com

Full list of author information is available at the end of the article

forebrain cholinergic compensation mechanisms. The results from this study reveal early changes in hippocampal activity prior to Aβ plaque deposition in AD. In addition, the current findings imply an important role of the cholinergic system to compensate for AD-related network alterations, thereby partially restoring sleep architecture and hippocampal activity.

Keywords Hippocampal local field potentials, REM sleep, NREM sleep, Sharp wave-ripples, Phase-amplitude coupling, TgF344-AD

Background

Sleep is a behavioral state characterized by relative loss of behavioral control and consciousness. During sleep, our body and brain cycle between two major phases; Non-rapid eye movement (NREM) sleep (75-80% of sleep duration and further subdivided in other sleep stages) that is marked by slow oscillations, and rapid eye movement (REM) sleep during which our body stays paralyzed but brain activity, breathing, heart rate and eye movements assimilate those during awake conditions. Sleep serves essential functions including the clearance of metabolites, waste-products, and toxic proteins, as well as promoting memory consolidation [47]. Sleep macro-architecture, which includes parameters such as sleep timing, sleep duration and the amount of time spent in different sleep stages, profoundly changes over the lifespan. Specifically, total sleep duration decreases, times of sleep shift, and the amount of REM sleep and NREM sleep decreases [55, 68]. Sleep disturbances are often observed in Alzheimer's disease, a progressive neurological disorder where the accumulation of toxic proteins, amyloid-beta (Aβ) and tau, lead to severe cognitive problems and behavioral deficits [39, 41]. AD patients commonly suffer with decreased amounts of REM and NREM sleep, as well as an increased number of awakenings, which interfere with the normal function of sleep, thereby promoting protein aggregation and hampering memory function [17].

Brain regions and pathways important for sleep and wake regulation [10], such as the cholinergic system [88] and locus coeruleus [86], are affected early by Aβ and tau accumulation [8, 9, 87]. Moreover, Aβ-induced neuronal hyperactivity has been linked to sleep-wake disturbances in several amyloid models of AD and in a recent study in AD patients [56]. Recent studies have demonstrated that soluble Aβ interferes with sleep regulation inducing increased or decreased wakefulness depending on the oligomer species present in the brain [48, 63]. In addition, several studies have observed changes in sleep macro-architecture and brain activity during sleep (sleep micro-architecture), at asymptomatic stages of AD in humans [40] and animal models of AD [67, 91]. Under physiological circumstances the sleep-wake cycle modulates Aβ levels in the interstitial fluid and cerebrospinal fluid [52]. Neuronal activity increases the generation and release of Aβ [19], leading to increased extracellular Aβ levels during wakefulness. Conversely, Aβ is cleared from the interstitial fluid during sleep by the enhanced activity of the glymphatic system [94]. These observations suggest a bidirectional link between sleep loss and Aβ accrual, wherein altered sleep macro-architecture (e.g. decreased total sleep time, decreased amount of NREM sleep and sleep fragmentation) results in increased extracellular Aβ levels and aggregation, which in turn further disrupts sleep, therefore, driving AD progression [67]. Moreover, subtle changes in brain activity during sleep have been observed, which are tightly linked to memory functions, such as decreased occurrences of slow oscillations [17, 50] and altered neural activity within the hippocampus, a key brain region involved in memory processes [24].

Hippocampal neuronal activity during sleep underlies memory consolidation through specific, coordinated electrophysiological events such as sharp wave-ripples (SWR) and theta-gamma coupling. SWR during NREM are considered a key mechanism for memory consolidation during which the excitatory input from the CA3, as reflected by the sharp wave, induces fast local oscillations (ripples) in the pyramidal layer of CA1 region [12]. Several studies observed altered properties of SWR in various mouse models of AD, which displayed decreased SWR power, decreased SWR frequency and reduced occurrence of ripples (for a review [70]). Theta-gamma coupling, mainly during REM sleep is another important oscillatory feature implied in memory consolidation and synaptic plasticity [5, 21]. The modulation of different gamma bands, namely slow gamma (30–60 Hz) and fast gamma (60–130 Hz) is postulated to reflect different memory processes. Studies have demonstrated that theta-slow gamma coupling oscillations is enhanced after successful retrieval of memories in humans [59] and rodents [37, 80, 81]. Instead, phase amplitude coupling (PAC) between theta and high gamma (60–130 Hz) is thought to be important for sensory processing and memory encoding [3, 6, 60]. Alterations in theta- fast gamma coupling have also been observed in people suffering from mild cognitive impairment (MCI) or advanced AD. MCI patients demonstrated with decreased theta- fast gamma coupling, which was correlated with decreased memory performance, and which further declined in patients with AD related dementia [32].

Hippocampal oscillations rely heavily on the delicate interplay of GABA-ergic, glutamatergic and cholinergic

neurotransmission [1, 12, 15, 22, 30]. A recent study observed changes in oscillatory activity and brain connectivity at early symptomatic stages of AD during sleep [56]. We hypothesize that perturbations of neurotransmitter systems due to the early accumulation of soluble Aβ, prior to Aβ-plaque accumulation and the symptomatic stages of AD, could disrupt brain oscillations during sleep. Studies in mouse models of AD have demonstrated that AB induced synaptic dysfunction induced alterations in neural activity during sleep [46, 97, 100]. However, knowledge on the extent of macro- and microstructural changes of sleep during early, presymptomatic stages of AD is limited. Moreover, insights into the neurological and synaptic mechanisms involved in these disturbances are lacking.

In this study, we aimed to assess hippocampal oscillatory activity during sleep at pre- and early-plaque stages of AD. To this end, we have performed 24-hour hippocampal electrophysiological measurements in 4-month-old TgF344-AD rats, displaying soluble Aβ pathology in the absence of Aβ plaques, and 6-month-old TgF344-AD rats demonstrating hyperphosphorylated tau accumulation in the locus coeruleus and hippocampal and cortical Aβ plaques [84]. Moreover, we aimed to evaluate the contribution of AD-related neuropathological changes in synaptic density to changes in hippocampal oscillatory activity. Hence, histological analyses of GABA-ergic, glutamatergic and cholinergic synapses in the hippocampus were performed to investigate possible disease mechanisms contributing to the alterations in hippocampal activity during sleep.

Materials and methods

Experimental design, animals, and ethical statement

To evaluate hippocampal dysfunction and sleep disturbances during early stages of AD, cross-sectional electrophysiological experiments were performed. All procedures were in accordance with the guidelines approved by the European Ethics Committee (decree 2010/63/EU) and were approved by the Committee on Animal Care and Use at the University of Antwerp, Belgium (approval number: 2019-06). Electrophysiological experiments were performed in 4-, and 6-month-old TgF344-AD male rats ($N=6/N=5$) and wildtype (WT) male littermates ($N=5/N=5$). These timepoints were based on previously performed histological analyses, which demonstrated increased concentrations of soluble Aβ-species in TgF344-AD rats, in the absence of Aβ-plaques in 4-month-old TgF344-AD rats [84]. Therefore, we name the 4-month-old timepoint the pre-plaque stage. At 6 months of age, Aβ-plaques were observed in the cortex and hippocampus of all TgF344-AD rats, hence naming this the early-plaque stage (Suppl. Figure 1).

Rats were group housed prior to the electrode implantation but housed separately afterwards. All animals were kept on a reversed, 12 h light/dark cycle, with controlled temperature (20–24 °C) and humidity (40–60%) conditions. Standard food and water were provided ad libitum and cage enrichment was provided to each animal. An additional 24 male rats were used for histological analysis of pathology and synaptic markers (6 WT and 6 TgF344-AD rats for each time point).

Chronic hippocampal electrophysiological measurements

Surgical procedure

Anesthesia was induced using 5% isoflurane (Isoflo ®, Abbott Laboratories) (medical air 1 L/min) and maintained using 2–3% isoflurane (at 1 L/min) during the surgery. Animals were placed in a stereotaxic frame and a craniotomy was made above the right dorsal hippocampus (AP -3.00, ML 2.50). A 16-channel laminar electrode (E16 + R-150-S1-L6 NT, Atlas Neuro-engineering) with internal reference was carefully lowered (DV 2.5–3.5 mm) into the dorsal hippocampus and the pointy tip feature of the electrode will penetrate the dura without damaging the dura. The exact depth of the recording sites was identified online by the layer-specific local field potentials (LFP) of the hippocampus. The craniotomy was sealed with a sterile silicon gel (Kwik-Cast, WPI). Stainless steel screws were drilled into the skull overlaying the olfactory bulb, frontal cortex, left hippocampus, and cerebellum, of which the latter served as ground electrode. The implant was covered in several layers of dental cement (Stoelting) and the wound was closed. Rats were treated with antibiotics until three days after the surgery (5 mg/kg, Enrofloxacin (Baytril®, Bayer) (in drinking water) and analgesics were administered (0.05 mg/kg Buprenorphine (Temgesic®, Indivior Europe Limited) subcutaneous during surgery, followed by 2 daily injections of 5 mg/kg Carprofen (Rimadil®, Pfizer) for two days after surgery. Rats were allowed to recover for at least 7 days prior to the LFP recordings.

Neurophysiological data acquisition

Prior to the recordings, all animals were habituated for 24 h to the ventilated, light-regulated recording chamber and recording setup. Using a wireless electrophysiology system (W2100 system, Multichannel systems), electrophysiological signals (LFPs, neuronal spiking activity, and EMG activity) were acquired for 24 h while the animal was freely behaving or sleeping in its home cage. During these measurements, animals were maintained on the 12/12 h reversed light/dark cycle and had ad libitum access to food and water.

Validation of electrode position

Anesthesia was induced with 5% isoflurane and was maintained at 2-2.5%. An electrical current (30μA, 3s) was applied via the electrode at the top, middle, and bottom channels to allow validation of the electrode position. Thereafter, the animals were euthanized via intravenous injection of 50 mg/kg pentobarbital (Dolethal ®, Vetoquinol, Belgium), followed by cardiac perfusion with ice-cold phosphate-buffered saline (PBS) and 4% Paraformaldehyde (Merck Millipore, Merck KGaA). The brains were surgically removed and postfixed for 4–6 h using 4% PFA. A sucrose gradient was applied (5%, 10%, and 20% Sucrose in 0.1 M PBS), after which the brains were snap frozen using liquid nitrogen and stored at -80 °C until further processing. The frozen brains of the animals were sliced into 12 μm thick coronal sections using a cryostat (Cryostar NX 70, Thermo Fisher Scientific). The sections were stained with Nissl staining (Cresyl Violet 0.1%, Sigma-Aldrich) and studied under the light microscope to validate the position of the electrodes for each animal.

Each layer of the hippocampus has distinct functions and therefore, distinct oscillatory activity. The focus of this study is on the different layers of the CA1 region. Therefore, histological electrode validation was performed. Based on the location of the tip of the electrode, and the applied lesions in the top, middle and bottom channel of the laminar electrode (Suppl. Figure 1), we could infer which channels were placed in the different layers of CA1. These channel locations were further validated by the distinct oscillatory patterns of the different hippocampal layers, such as occurrence of sharp wave-ripples and theta power across different hippocampal layers. This channel information was used in further analyses. For 2 WT animals and 2 Tg animals, histological validation was not possible because the lesions were not visible under the microscope and are not shown in the figure. However, based on distinct oscillatory patterns, mainly the presence of sharp wave ripples and locating the channels with the maximum amplitude of theta oscillations, channel location in three out of four animals could be inferred [13]. Hence, these animals were included in the data analysis. One 4-month-old transgenic animal was excluded from the hippocampal oscillatory analysis due to bad signals in the majority of the channels.

Analysis

Sleep architecture and fragmentation

An automated sleep scoring algorithm was used to determine vigilance states for each 10 s epoch based on the theta-delta ratio and EMG activity. Each 10 s epoch was labeled as wake, REM or NREM. Next, the automatic sleep scoring was checked and adjusted through visual inspection by two independent investigators. The scores of the two investigators were combined to a single score per animal that was used in our further analysis of sleep architecture. The percentage time spent in each vigilance state was calculated in 3 h time periods across the 24 h recording and sleep bout lengths during the light (inactive phase, start Zeitgeber 0) and dark (active, start Zeitgeber 12) phase of the day were derived to evaluate sleep fragmentation. Mean sleep bout lengths during the active and inactive phase and over the entire 24 h period were calculated for each subject. The individual sleep bout lengths were used in a second analysis to create a cumulative probability plot and Kolmogorov-Smirnov tests (FDR corrected $p < 0.05$) were used to evaluate differences in sleep fragmentation between genotypes.

Power analysis of hippocampal LFPs

For each channel on the electrode, power spectra were calculated for each vigilance state using a Fast Fourier Transform in Brainstorm [79] using the Welch's method (window size 20s, 50% overlap). Power spectra were normalized to the sum of the power across all LFP frequencies (0.5–250 Hz) to minimize variation in amplitude due to differences in the exact placement of the electrode. Normalized power spectra were averaged across genotypes separately for each state. Next, power for each vigilance state was calculated for specific frequency bands of interest, i.e., delta (0.4–4 Hz), theta (5–12 Hz), slow gamma (30–45 Hz), fast gamma (60–120 Hz) and sharp wave- ripple (120–250 Hz). The power across the three channels with the highest power at each frequency was averaged for each subject and compared between groups and ages.

Phase-Amplitude coupling (PAC)

The amplitude of the hippocampal gamma rhythm is modulated by the phase of theta, a phenomenon named phase-amplitude coupling (PAC). To evaluate the strength of the theta-gamma coupling, the modulation index (MI) was used, that after bandpass filtering uses the phase of the slow oscillation and the amplitude envelope of the fast oscillation, to create a complex vector of which the length represents the amplitude of each fast oscillation whereas the phase of the slow oscillation is represented by the angle. In the case of an absence of PAC, these vectors form a roughly uniform circular shape centered around zero, however, if there is modulation, then the amplitude at a certain phase is higher, which will create a bump in the polar plot. The MI represents the length of this mean vector length (for a detailed description of calculations we refer to [16, 82]). The analysis of the PAC was performed on one channel, which was located in the pyramidal layer of the CA1, based on histological electrode validation (described in Sect. 2.3). First,

for each subject, a comodulogram was calculated which demonstrates the MI for each pair of frequencies. The theta band (5–12 Hz) and gamma band (30–120 Hz) were divided into 1 Hz bins and for each combination of theta and gamma frequencies the mean modulation index across each REM epoch was calculated and averaged across all REM epochs to create a subject-based comodulogram. Next, a group-averaged comodulogram was computed in Matlab which demonstrated for each group the main frequencies of modulation. The main frequency modes of modulation were examined and were used to perform a time-resolved PAC (tPAC) analysis. tPAC computes the MI between specific frequency bands estimated from the group-averaged comodulogram for each 1-second epoch. The advantage of this method is that it allows a more reliable quantification of the strength of the PAC. The obtained MI were averaged across epochs for each subject and the mean was statistically compared between groups and ages.

Offline detection and analysis of Sharp wave-ripples

All preprocessing steps were conducted using the Fieldtrip toolbox [62]. First, to detect ripples in the pyramidal layer of CA1, the wide-band signal was band-pass filtered between 120 and 250 Hz using a 400th order Butterworth infinite response filter and was afterwards down-sampled to 1200 Hz. Filtered data was segmented based on the NREM epochs obtained in Neuroscore. The segmented data was z-scored, rectified and smoothed using a rectangular filter window with a length of 8ms, generating the ripple power signal [57]. SWR were identified in the channels which were placed in the pyramidal layer of the CA1, based on the electrode validation described in 2.3.1. If the power within the ripple band exceeded a threshold of 4 standard deviations from the mean. Events were expanded until the power fell below 2 standard deviations and events with a duration shorter than 30ms and/or a peak spectral frequency lower than 140 Hz were discarded. Subsequently, a thresholding algorithm was applied to detect sharp waves in the stratum radiatum. Signals in the channel that demonstrated strong sharp waves were band-pass filtered between 0.5 and 20 Hz using a 400th order Butterworth filter. Sharp wave (SW) events which lasted between 20ms and 400ms were detected when the power of the filtered signal exceeded the threshold of 2.5 standard deviations from the mean [61]. Ripples that co-occurred with SW were kept for further analysis. The power in the SWR band, the peak spectral frequency and the duration of events were extracted and compared between groups and ages.

Table 1 Antibodies used for immunofluorescent stainings

Target	Supplier	Catalogue nr.	RRID	Dilution
vGAT	Synaptic Systems	131,003	AB_887869	1:200
vGLUT	Synaptic Systems	135,304	AB_887878	1:200
vAChT	Merck	ABN100	AB_2630394	1:1000
FITC AffiniPure™ Donkey Anti-Guinea Pig IgG (H + L)	Jackson ImmunoResearch	706-095-148	AB_2340453	1:400
Cy™5 AffiniPure™ Donkey Anti-Goat IgG (H + L)	Jackson ImmunoResearch	705-175-147	AB_2340415	1:800
CyTM3-conjugated Fab goat anti-rabbit IgG (GAR-Fab-Cy3)	Jackson ImmunoResearch	111-167-003	AB_2313593	1:2000

Histology

Immunofluorescence staining

To evaluate AD alterations in synaptic markers, histological analyses were performed on cryosections as described in [84]. Briefly, brains were extracted, and hemispheres were separated. Next, left hemispheres were embedded in OCT-embedding medium for sectioning. At 0.4, 1.40- and 3.90-mm lateral from the midline, sagittal sections of 12 µm were made using a Leica CM1950 cryomicrotome (Leica BioSystems, Belgium), thaw-mounted on VWR Superfrost Plus micro slides (VWR, Leuven, Belgium) and dried for 2 h at 37 °C. All immunohistochemical incubations were carried out at RT. Sections were pre-incubated for 30 min in blocking buffer containing 1% Triton X-100 before an overnight incubation with the primary antibodies (Table 1). For the detection of the immunoreactivity, the sections were incubated for 4 h with the appropriate combination of fluorescent-conjugated secondary, followed by a nuclear counterstain using 4′,6-diamidino-2-phenylindole (DAPI, Sigma-Aldrich, Hoeilaart, Belgium) for 10 min at room temperature. Samples were mounted in Citifluor AF1 (EMS, Hathfield, USA). Respective single-labeling studies which resulted in comparable staining, were performed to rule out non-specific findings resulting from the multiple-staining process. Negative staining controls were performed by substitution of non-immune sera for the primary or secondary antisera.

Image acquisition

Confocal images of immunolabeled tissue sections were acquired with a Perkin Elmer Ultraview Vox dual

spinning disk confocal microscope, mounted on a Nikon Ti body using a 40x Plan Apo objective (NA 0.95). Lasers with wavelength 405 nm, 488 nm, 561 nm and 640 nm were used in combination with a quadruple dichroic and 445/60–525/50–615/70–705/90nm emission filters. Detection was done on a Hamamatsu C9100-50 CMOS camera. Image acquisition was done using Volocity software. Regions of interest were localized based on the DAPI staining. Per animal, 3 images were acquired on 3 non-consecutive sections in 3 axial positions separated by a 2 µm spacing.

Image analysis

Image analysis of the synaptic excitatory/inhibitory ratio was done in FIJI image analysis software [72] as described in [84]. A macro script was written for FIJI image analysis software [1] to detect synaptic markers and measure their intensity and is available on github (https://github.com/DeVosLab/SynapseDetection) [89, 90]. After max imum projection of the Z-stacks, synaptic marker spots were enhanced using a single or multi-scale Laplace filter with user-defined kernel sizes. For each marker, the threshold settings were kept constant for both rat groups and age categories studied (Table 2). A manually defined threshold per region was applied to segment the spots after which an additional max finding (and region growing) step was included to untangle clustered spots. Only spots that had a projected area within a specific range (0.20–3.00 µm) were retained. Images with more than 10,000 spots were discarded to exclude over segmented images ($N = 8$, 5,56%).

Statistics

The statistical analysis of the data was performed using the JMP Pro software (Version 16, SAS Institute Inc., Cary, NC, 1989–2021). For the statistical analysis of the sleep architecture, circadian rhythmicity, power across different frequency bands, SWR characteristics, and PAC, outlier detection was performed across all samples, using principal component analysis (PCA). Measurements with a Hotelling T^2 statistic index, which the square of the Mahalanobis distance, higher than the 95% confidence interval were excluded. Two-way ANOVA's (genotype, age, genotype*age) were performed, and multiple comparison correction was applied on the ANOVA outcomes (False discovery rate (FDR) correction using Benjamini-Hochberg procedure). In case of a significant genotype*age interaction, post-hoc Student's t-tests were performed. An FDR correction was again applied to correct for multiple comparisons in the post-hoc analyses (FDR $p < 0.05$). Moreover, the Cohen's d coefficient was calculated as a measure of effect size. The interaction term was removed if no significant interaction was observed, and a two-way ANOVA (genotype, age) was used to evaluate genotype or age effects.

Regarding the analysis of the synaptic markers, outlier detection was performed using the interquartile range (1.5x IQR) per genotype, age, and region on all individual images (3 per animal). Animals with less than 2 images were excluded and the remaining images were averaged for each animal. A second outlier detection was performed on the subject averages, using principal component analysis, using the criteria described earlier. A two-way ANOVA (genotype, age, genotype*age) per region was used to evaluate differences in vGLUT/vGAT ratio and the number of cholinergic synapses. In case of a significant genotype*age interaction, post-hoc FDR-corrected Student's t-test (FDR $p < 0.05$) were performed. The interaction term was removed if no significant interaction was observed, and a two-way ANOVA (genotype, age) was used to evaluate genotype or age effects. Graphical representation of the data was obtained using GraphPad Prism (version 9.2.0 for Windows, GraphPad Software, San Diego, California USA, www.graphpad.com).

Results

Evaluation of circadian rhythmicity and sleep macro-architecture in TgF344-AD rats

Total sleep time is known to decrease while aging, a decline which is exacerbated in AD [17, 98]. Upon examination of total time spent in REM, NREM or wake over 24 h, we did not observe significant age, nor genotype effects (Fig. 1A., Suppl. Table 1). Moreover, when evaluating time spent in each vigilance state across the inactive (lights on) (Fig. 1B, Suppl. Table 2) and active (lights off) (Fig. 1C, Suppl. Table 3) phase, we did not observe significant effects, suggesting that robust changes in sleep macro-architecture are absent in TgF344-AD rats at early stages of AD.

Next, we aimed to investigate if more subtle changes were present by dividing the 24-hour acquisitions into

Table 2 Threshold settings fluorescent image analysis

	CA1			DG		
	vGlut	**vGAT**	**vAChT**	**vGlut**	**vGAT**	**vAChT**
segmentation method	Multi-scale	Multi-scale	Multi-scale	Multi-scale	Multi-scale	Multi-scale
Gauss/Laplace scale	2	1	1	2	1	1
Fixed threshold	7	2	3	7	3	3
Max Scale Multi	3	3	3	3	3	3

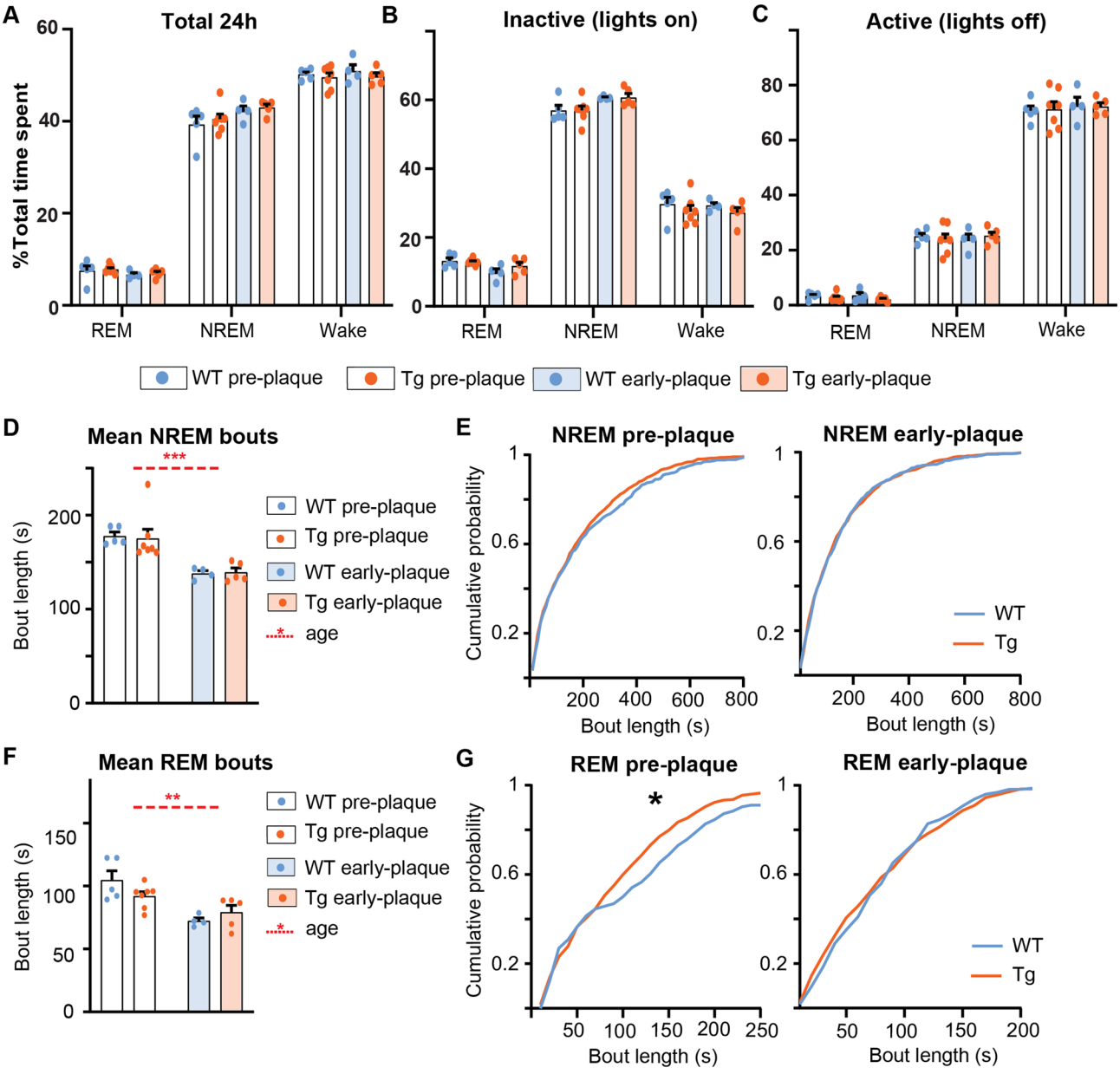

Fig. 1 Sleep macroarchitecture in TgF344-AD rats. **A**-**C**) Percentage time spent in REM (left) NREM (middle) and wake (right) during the total 24-hour acquisition (**A**) and during the inactive (**B**) and active phase (**C**). **D**-**F**) Mean NREM (**D**) and REM (**F**) bout lengths across 24 h. Bars represent the mean +/- SEM. ANOVA analysis was performed to test for statistical differences. **E**-**G**) Cumulative probability plots of NREM bout lengths (**E**) and REM bout lengths (**G**) for all animals within each group. The left panel shows the cumulative distribution during the pre-plaque stage, while the right plot shows the early-plaque stage. Kolmogorov-Smirnov tests (FDR $p < 0.05$) were performed to evaluate if distributions were significantly different. s = seconds, WT = wildtype, Tg = TgF344-AD, * = $p < 0.05$, ** = $p < 0.01$, *** = $p < 0.001$

3-hour bins and plotted the percentage time spent in each vigilance state across each time bin (Suppl. Figure 2). No age, nor genotype effects were observed in the time spent in REM sleep (Suppl. Figure 2 A, Suppl. Table 4). During NREM sleep, we observed a genotype*age interaction during Z9-Z12, which is at the end of the inactive phase (Suppl. Figure 2B, Suppl. Table 5). Post-hoc analysis revealed a significant genotypical difference at the pre-plaque stage, with TgF344-AD rats spending significantly less time in NREM compared to WT littermates (Suppl. Table 6). This difference was not present at the early-plaque stage, where NREM time decreased over time in WT whereas NREM time was increased in the TgF344-AD rats over time. These changes in time spent in NREM were also reflected in the time spent awake, where a similar genotype*age interaction was observed during Z9-12, demonstrating a significantly higher percentage of time spent awake in TgF344-AD rats at the

pre-plaque stage. Note that given we found no significant changes for REM, wake and NREM are anticorrelated. Moreover, there was a significant increase in wakefulness in WT rats at the early-plaque stage (Suppl. Figure 2 C, Suppl. Tables 7, 8), demonstrating that the observed effects are dominated by changes in WT rats.

During aging, sleep becomes more fragmented, meaning a higher occurrence of awakenings and therefore, decreased sleep bout lengths. To investigate if TgF344-AD rats display sleep fragmentation, average duration of NREM and REM bouts were calculated for each subject (Suppl. Figure 3) and compared across groups (Fig. 1D, F). Statistical analysis did not reveal significant genotypical differences in NREM nor REM bout length between groups. However, for both REM and NREM bout length, age effects were observed, showing a decreased mean bout length at the early-plaque stage, irrespective of genotype (Suppl. Table 9). These results confirm our previous observation that no major changes in sleep macro-architecture are present in TgF344-AD rats at these early stages.

To evaluate subtle AD-related differences in bout length, NREM and REM bout lengths of all subjects were combined in cumulative probability plots for each animal (Suppl. Figure 2) and for each group (Fig. 1E, G). NREM bout length between WT and TgF344-AD rats at pre- and early-plaque stages of AD was not significantly different ($p_{pre-plaque}$ = 0.0832, $p_{early-plaque}$ = 0.4728, Kolmogorov-Smirnov) (Fig. 1E). However, a significantly increased probability of shorter REM bouts, a signature of increased REM sleep fragmentation, was observed in TgF344-AD rats at the pre-plaque stage, but not at the early-plaque stage ($p_{pre-plaque}$ = 0.0400, $p_{early-plaque}$ = 0.2958, Kolmogorov-Smirnov) (Fig. 1G). To summarize, only subtle differences in sleep macro-architecture were observed in TgF344-AD rats at the pre-plaque stage, but not at the early-plaque stage.

Alterations in sleep microarchitecture during NREM sleep

Most of the studies on sleep in AD have focused on alterations in brain activity during NREM sleep (sleep micro-architecture). Aβ and hyperphosphorylated tau have been known to interfere with synaptic function, hence inducing altered oscillatory activity during NREM sleep, which in turn is linked to cognitive symptoms of AD [33, 53]. When investigating the oscillatory power during NREM sleep in TgF344-AD rats, no significant genotype effects were observed in the power across different frequency bands (Fig. 2A, B, Suppl. Table 10). However, a significant age effect was observed in the delta band, demonstrating a decreased power at the early-plaque stage, irrespective of genotype.

Next, to investigate if more refined alterations in sleep micro-architecture were present, SWR activity was already altered at pre-plaque and early-plaque stages of AD in the TgF344-AD rats, SWR were extracted (Fig. 2C, cfr. Materials and Methods) and power, peak spectral frequency (PSF) and duration of SWR were examined (Fig. 2D, Suppl. Table 11). No significant genotype, nor age effects were observed for the power of the SWR PSF of the SWR (Fig. 2E). However, a genotype effect was observed in the duration of the SWR, demonstrating a significantly increased duration of SWR in the TgF344-AD rats, irrespective of age (Fig. 2F). Histograms of the relative frequency for each duration of SWR demonstrated a skewed distribution, which was not significantly different between WT and TgF344-AD rats (Kolmogorov-Smirnov, FDR $p < 0.05$) nor across ages ($p_{pre-plaque}$ = 0.6994, $p_{early-plaque}$ = 0.998) (Fig. 2G). Next, all SWR events were divided into short ripples (< 60 ms), medium ripples (60–100 ms) and long ripples (> 100 ms), as described in [29]. Statistical analysis was performed to evaluate if the increased duration was due to a shift in the balance between SWR duration. The results demonstrated an increased fraction of long ripples (Fig. 2H, Suppl. Table 12) in the TgF344-AD rats, in the absence of genotypical differences in short and medium duration ripples, showing that the relative number of long duration ripples is increased at pre- and early-plaque stages of AD in the TgF344-AD rats (Fig. 2H).

Hippocampal excitatory/inhibitory balance in TgF344-AD rats

SWR events are induced by a delicate interaction between excitatory neurons and GABAergic interneurons that, if disrupted, can lead to pathological forms of activity which leads to memory impairments [4, 26, 70, 99]. Therefore, we aimed to evaluate if altered excitatory or inhibitory balance could be attributing to the increased SWR duration observed in TgF344-AD rats (Fig. 3A). Analysis of the excitatory/inhibitory balance (ratio between glutamatergic and GABA-ergic synapses) revealed no significant genotype, nor age effects in the CA1 layer and dentate gyrus of the hippocampus (Fig. 3B, Suppl. Table 13).

Alterations in sleep microarchitecture during REM sleep

Next, we aimed to assess if oscillatory activity during REM sleep was affected at pre-plaque and early-plaque stages of AD. When investigating alterations in the power of hippocampal oscillations during REM sleep, no significant genotype effects, nor age or interaction effects were observed in delta, low theta, high theta, slow gamma, and fast gamma power in the TgF344-AD rats (Fig. 4A, B, Suppl. Table 14).

Alterations in synaptic function could impair theta-gamma coupling, therefore we evaluated PAC during REM sleep. First, the main frequencies modulated by

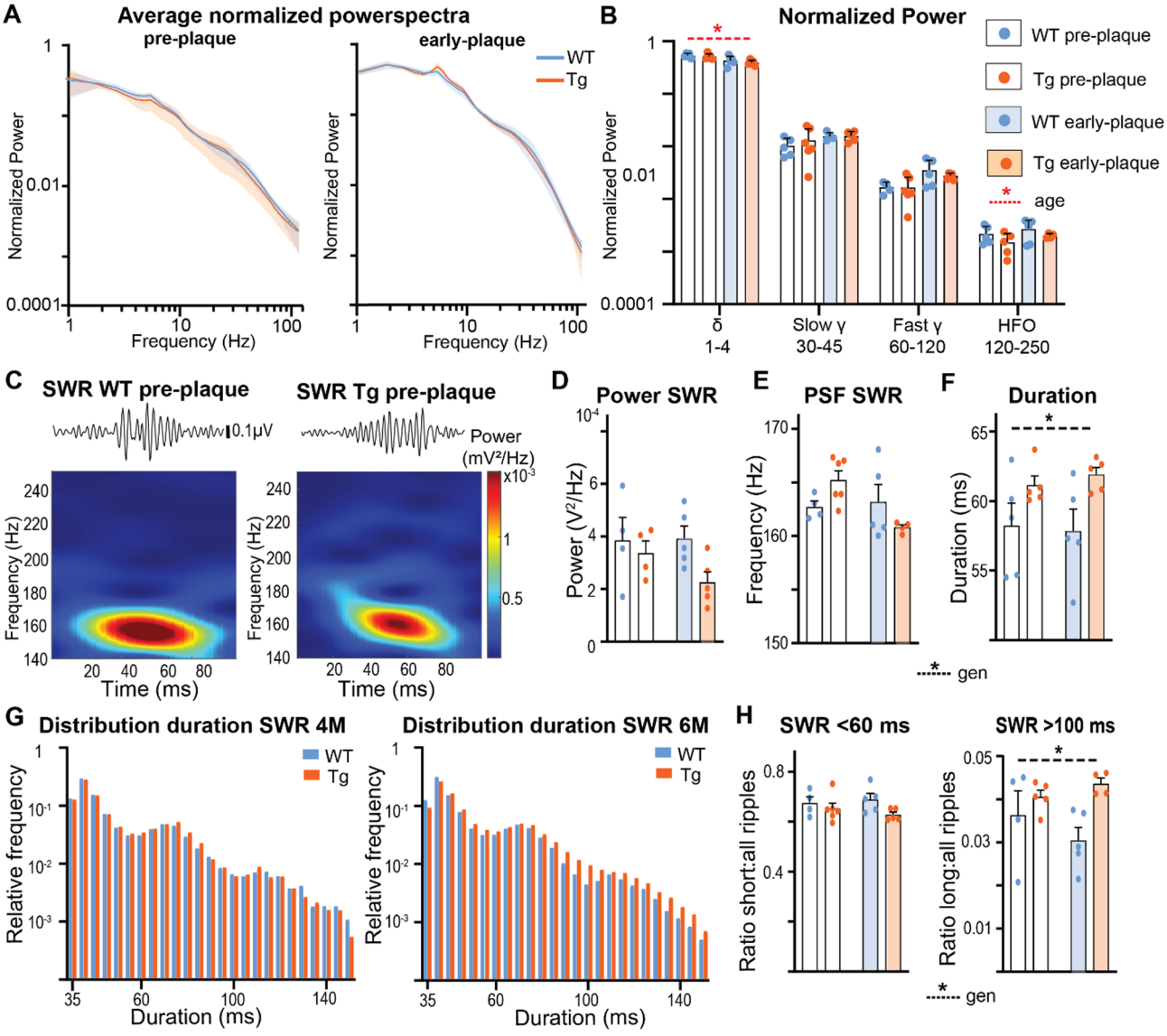

Fig. 2 Power and sharp wave-ripple activity during NREM sleep in TgF344-AD rats and wildtype littermates. **A**) Mean normalized power spectra during NREM sleep. Shading indicates SEM across the group. **B**) Averaged normalized power across distinct frequency bands of interest (+/- SEM). **C**) Illustrative sharp wave-ripple (SWR) of a wildtype (WT) and TgF344-AD (Tg) rat. Trace shows filtered data (120–250 Hz) of the ripple, while the bottom time-frequency plot demonstrates the frequency and power of the ripple. **D**-**F**) Bar plots demonstrating the mean power (**D**), peak spectral frequency (**E**) and duration (**F**) of SWR. **G**-**H**) Histograms showing the group average relative frequency of each duration of SWR at the pre-plaque stage (left) and early-plaque stage (right). **H**) Bar plots showing the ratio of short ripples (left) and long ripples (right) vs. all ripples. Bar plots show mean +/- SEM, whereas dots represent subject values. gen = genotype, HFO = high frequency oscillations, ms = millisecond, PSF = peak spectral frequency, Hz = Herz, V = Volt. * = $p < 0.05$

theta frequencies were identified using a comodulogram. Mean comodulograms were plotted which demonstrate modes of coupling between theta frequencies (6.5–9 Hz) and fast gamma in all groups (80–100 Hz) (Fig. 4C). Interestingly, strong coupling was observed between theta (6.5–9 Hz) and slow gamma oscillations (30–45 Hz) mainly at the pre-plaque stage in TgF344-AD rats.

Next, to evaluate the strength of the theta-gamma coupling, a time-resolved PAC analysis was performed (Fig. 4D, E, Suppl. Table 15). A significant age*genotype interaction was observed in the coupling between theta and slow gamma frequencies. Post-hoc analysis revealed increased coupling strength in TgF344-AD rats during the pre-plaque stage, which however was normalized back to WT levels at the early-plaque stage indicating potential processes leading to a temporary (at least) restoration (Fig. 4D, Suppl. Table 16). When evaluating the coupling between theta and fast gamma frequencies, a significantly decreased coupling strength was present in the TgF344-AD rats, irrespective of age (Fig. 4E, Suppl. Table 15). Moreover, a significant age effect was observed, demonstrating an increase in the strength of

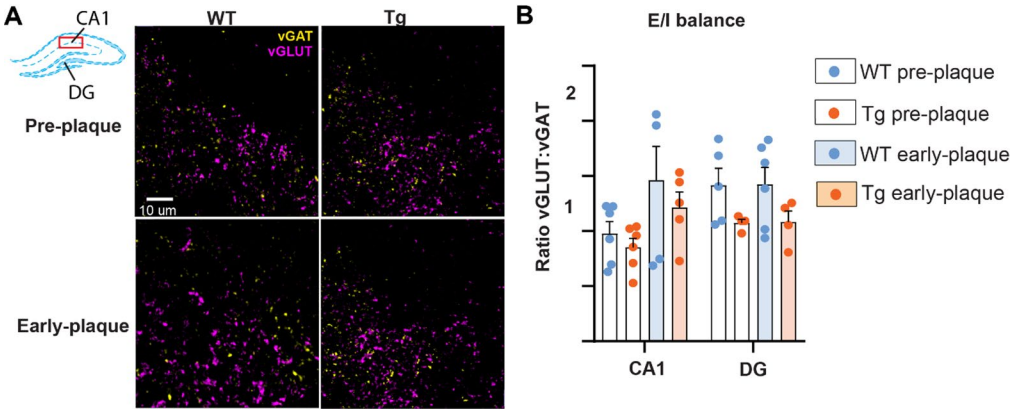

Fig. 3 Changes in E/I balance in TgF344-AD rats. **A**) Exemplary images of the glutamatergic (magenta) and GABA-ergic (yellow) synapses in the CA1 layer of the hippocampus in wildtype littermates (WT) (left) and TgF344-AD rats (right) at the pre- and early-plaque stage. **B**) Group-averaged vGLUT/vGAT ratio per region of interest. Bars represent the mean +/- SEM. ANOVA analysis was performed to test for statistical differences. DG = dentate gyrus, vGAT = vesicular GABA transporter, vGLUT = vesicular glutamate transporter, E/I = excitatory/inhibitory

PAC in the 6-month-old rats, which is mainly driven by an increasing MI in the TgF344-AD rats over time, suggesting a partial recovery of PAC in TgF344-AD rats at the early-plaque stage.

Cholinergic synapses in the hippocampus

To evaluate if the observed alterations in theta-gamma coupling could be attributed to alterations in cholinergic function, histological analysis of cholinergic synapses in the hippocampus was performed (Fig. 5A). When statistically comparing the abundance of cholinergic synapses, significant genotype*age effects were observed in the DG and in the CA1 (Fig. 5B, Suppl. Table 17). Cholinergic synaptic density in the CA1 region and DG was paradoxically increased at the early-plaque stage in TgF344-AD rats compared to WT littermates suggesting a potential compensation mechanism. Moreover, a significant increase in cholinergic synapses was observed over time in the TgF344-AD rats in both hippocampal regions, which was absent in WT littermates. This, together with the normalization of the coupling between theta and slow gamma in the TgF344-AD rats at this time point (see previous section), is suggestive of a compensatory mechanism occurring in TgF344-AD rats at the early-plaque stage (Fig. 5B, Suppl. Table 18).

Discussion

The current study aimed to evaluate how hippocampal oscillatory activity during sleep is altered at pre-plaque and early-plaque stages of AD in TgF344-AD rats and to elucidate the contribution of AD-related altered synaptic signaling to the changes in hippocampal activity. When investigating properties of SWRs during NREM, we observed an increased ripple duration in TgF344-AD rats, mainly at the early-plaque stage, while the power of the oscillations and peak spectral frequency was not significantly different between genotypes. During REM sleep, a significantly decreased PAC between theta and fast gamma oscillations was observed in the TgF344-AD rats at both ages. Interestingly, at the pre-plaque stage in TgF344-AD rats, a significant increase in PAC was present between theta and slow gamma oscillations, which was absent at the early-plaque stage, demonstrating a partial normalization of hippocampal function during the early-plaque stage in TgF344-AD rats. The aforementioned refined micro-architectural changes during NREM and REM sleep were observed in the absence of large micro-architectural changes, as power across different frequency bands was not affected. The alterations in oscillatory activity during sleep coincided with changes in synaptic density of cholinergic synapses, but not with changes in glutamatergic and inhibitory synapses. Interestingly, an increase of cholinergic synapses was observed only at 6 months of age in the hippocampus of TgF344-AD rats suggesting a relationship to the partial normalization in hippocampal oscillatory activity observed at this early plague stage timepoint. The changed alterations in hippocampal activity were observed in the absence of large changes in sleep macroarchitecture, where the amount of REM sleep and NREM sleep was not significantly different between genotypes, and signs of NREM sleep fragmentation were absent. We did observe a subtle hint towards REM sleep fragmentation in the TgF344-AD rats at the pre-plaque stage, but not the early-plaque stage.

Prior evidence of hippocampal dysfunction in TgF344-AD rats

TgF344-AD rats display progressive Aβ plaque accumulation in the cortex and hippocampus starting from 6 months of age [20, 84]. Our previous studies have demonstrated that at 4 months of age, increased

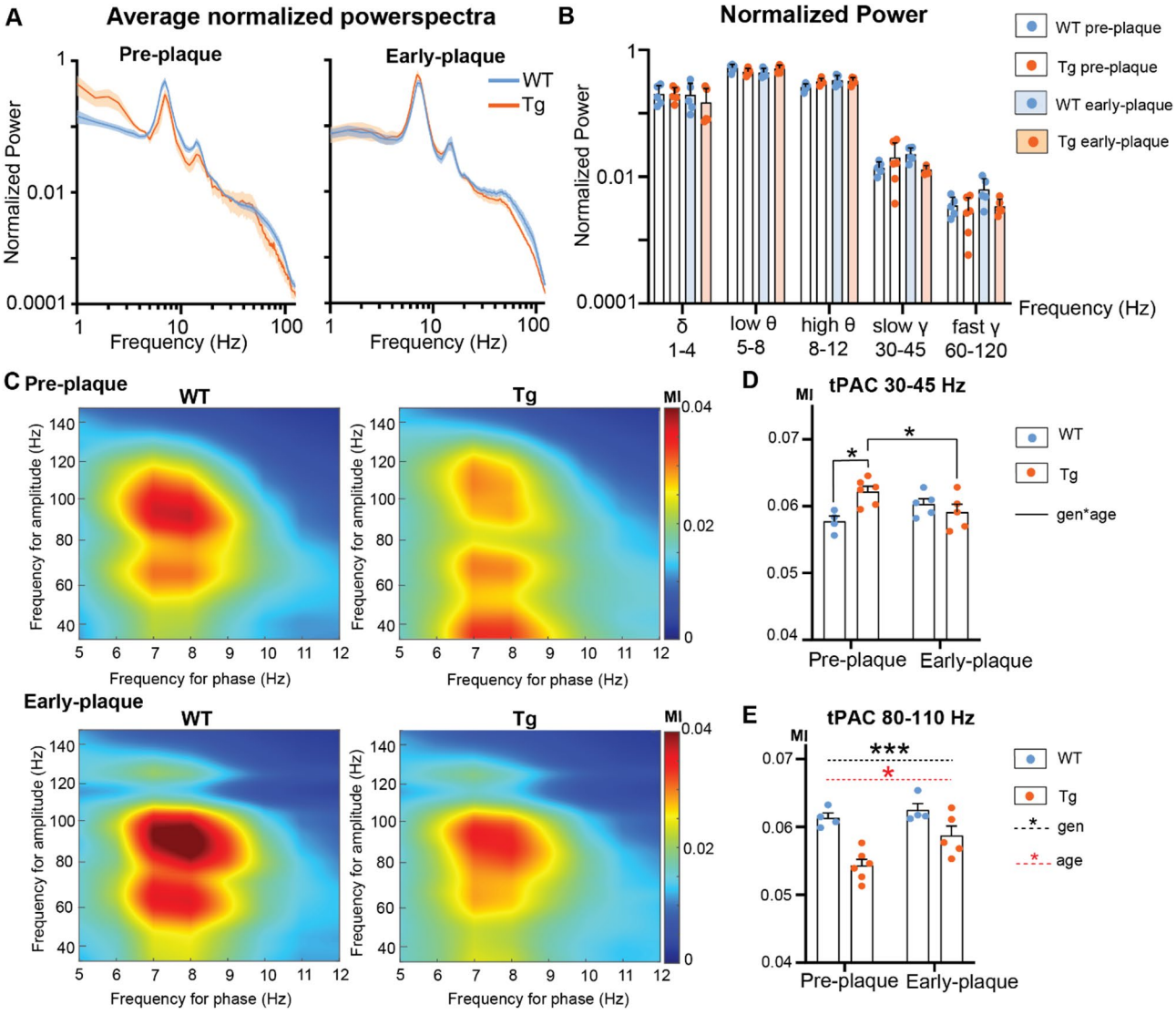

Fig. 4 Power and theta-gamma coupling in TgF344-AD rats during REM sleep. **A**) Mean normalized power spectra. Shading indicates SEM across the group. **B**) Averaged normalized power across distinct frequency bands of interest (+/- SEM). **C**) Comodulogram averaged across subjects demonstrating main frequencies of coupling. Color bar indicates the strength of the modulation index (MI) at different frequencies of theta (x-axis) and gamma (y-axis). **D**) Mean (+/- SEM) MI across subjects between theta-frequencies (6.5–9 Hz) and slow gamma frequencies (30–45 Hz). Dots represent subject MI values. **E**) Mean (+/- SEM) MI across subjects between theta frequencies (6.5-9HZ) and fast gamma frequencies 80–110 Hz. Dots represent subject MI values. gen = genotype, Hz = Hertz. * = $p < 0.05$, *** = $p < 0.001$

concentrations of soluble Aβ monomers and oligomers in the brains of TgF344-AD rats, in the absence of cortical and hippocampal Aβ plaques [66, 71, 84], resulting in aberrant neural activity as measured by resting state functional MRI [84] and altered hippocampal activity in rats performing an open field task or linear track [58, 85]. To our knowledge, our former and current study are one of the few electrophysiological examples performed at the pre-plaque stage in TgF344-AD rats as most electrophysiological studies in the TgF344-AD rats have been performed at older ages. These studies observed enhanced excitability of excitatory neurons in the Dentate Gyrus in 6-month-old male TgF344-AD rats [73, 74], decreased PAC in the cortex and hippocampus of 9- to 12-month old rats [2] and decreased rate of SWRs in 12-month old TgF344-AD rats [78].

Power of hippocampal oscillations

In clinical en preclinical studies, alterations in power of slow oscillations, theta oscillations and gamma oscillations have been observed during sleep, where the direction of the changes over the course of the disease [14, 44]. Longitudinal studies in AD mouse models reveal initial increases in power of slow wave- [18, 35], theta- [35], and gamma power [45], followed by a significantly decreased power in these frequencies at more advanced AD stages.

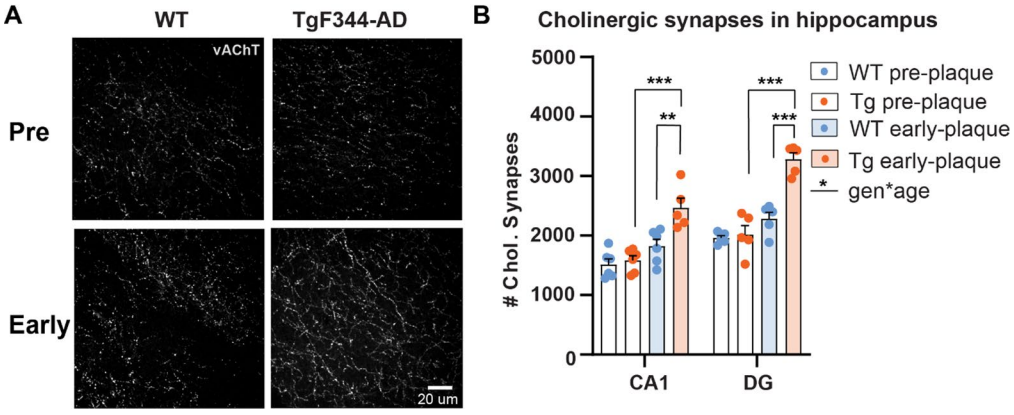

Fig. 5 Increased number of cholinergic synapses in hippocampus during early-plaque stage. **A**) Exemplary images of cholinergic synapses (grey) in the CA1 layer of the hippocampus in wildtype littermates (WT) (left) and TgF344-AD rats (Tg) (right) at the pre- and early-plaque stage of AD. **B**) Group-averaged numbers of cholinergic synapses per region of interest. Bars represent the mean +/- SEM. Dots represent subject MI values. ANOVA analysis was performed to test for statistical differences. If an age*genotype interaction is observed, the results of the post-hoc FDR corrected Students T-test are displayed. DG = dentate gyrus, gen = genotype. ** = $p < 0.01$ *** = $p < 0.001$

This contrasts with our current findings, where we do not observe genotypical differences in power of hippocampal oscillations during REM, nor NREM sleep. This could be explained by the early disease state we are investigating. Our previous electrophysiological studies in TgF344-AD rats behaving in an open field and linear track demonstrated decreased power in slow and fast gamma oscillations at 6-months of age and decreased theta-, and fast gamma power at 4-months of age [28, 85]. In contrast, in the current study we did not observe genotypical differences in oscillatory power in the hippocampus during REM, nor NREM sleep, despite the fact that the recordings were acquired in the same animals. This could in part be explained by the differential impact of behavioral state on hippocampal oscillatory activity [100]. Our results suggest that the refined changes in sleep microarchitecture observed at the pre-plaque stage, occur in the absence of large-scale disruptions of hippocampal activity during sleep.

Hyperexcitability of the hippocampal network

Previous studies in 6-month to 8-month-old TgF344-AD rats did observe an increased presence of cortical high voltage spindles (HVS), characterized as hypersynchronous, negative voltage 7–8 Hz spike–wave discharges. These HVS were only present during quiet wakefulness and were more pronounced in the frontal cortex and less pronounced in parietal cortex, while they were absent in the occipital cortex [78]. The current manuscript did not focus on the oscillatory activity during (quiet) wakefulness. However, a previous study observed early epileptiform activity in a mouse AD mouse models mainly during REM sleep [43]. Upon inspection of the REM sleep data, we did not observe pronounced epileptiform activity (interictal spikes, HVS) in the TgF344-AD rats, possibly due to the early stage of AD or, though unlikely, because of a lack of hyperexcitability in the hippocampal network. This is in line with our histological findings, which do not demonstrate a significant shift in E/I balance in the TgF344-AD rats. However, as a previous electrophysiological study on brain slices demonstrated increased excitability of neurons within the dentate gyrus of the hippocampus of 6-month-old TgF344-AD rats [74], a thorough analysis should be performed on the REM sleep data to completely exclude the presence of hippocampal epileptiform activity.

SWR disturbances

Sharp-wave ripples during NREM are considered a key mechanism for memory consolidation during which the excitatory input from the CA3, as reflected by the sharp wave, induces fast local oscillations (ripples) in the pyramidal layer of CA1 region [12]. Several studies observed altered properties of SWR in various mouse models of AD, which displayed decreased SWR power, decreased SWR frequency and reduced occurrence of ripples (for a review [70]). These alterations were mainly attributed to reduced inhibitory control of the hippocampal network [15, 93, 95]. Here, we did not observe genotypic alterations in power, nor spectral frequency of SWR in TgF344-AD rats, which can be the result of the different disease stage in the current study, since the aforementioned studies focussed on late-stage AD (e.g. late post-plaque stages). This is in line with the histopathological analysis showing that the excitatory/inhibitory balance is not altered in TgF344-AD rats, since changes in SWR have been linked to changes in inhibitory function [15].

However, we did observe a significantly increased duration of SWR in TgF344-AD rats, irrespective of age, which might be indicative of an increased memory

demand in AD [29]. Research indicates that learning and correct recall in spatial memory is associated with long duration SWRs. Moreover, prolongation of SWRs has been shown to improve working memory performance, whereas decreasing duration decreased performance. These results suggest that the observed change in the duration in the SWR might improve cognition. However, behavioral studies have demonstrated spatial memory impairment in 6-month-old TgF344-AD rats, suggesting that the increased SWR duration might not be beneficial [65]. Future research correlating cognition to the presence of long-duration SWRs at early stages of AD might provide novel insights regarding the role of SWR disturbances in cognition. In contrast, several studies have reported decreased duration of SWRs in AD mouse models. Reduced duration of SWRs has been noted in vivo in 12-month old anesthetized APP/PS1 mice [96] and in 9-month-old freely behaving APP/PS1 mice displaying extensive cortical and hippocampal amyloid accumulation and cognitive impairment from 6-month onward [42]. This decrease was also observed in vitro in hippocampal slices of 5xfAD mice [15]. On the other hand, no differences in SWR duration have been observed in freely behaving in 7-month old rTg4510 mice, a tauopathy model which show extensive neurodegeneration at this age [93]. Differences between animal models, stage of AD pathology, and experimental design may account for these inconsistent findings. Interestingly, the current observation of increased SWR duration during sleep is also different in comparison to our findings in a previous study in the same animal model and disease stage, where we observed a decrease in ripple duration of 4-month-old TgF344-AD rats during an exploratory task [85]. Hence, we conjecture that the differences may reflect that the observed alterations in SWR duration might also be dependent on behavioral state [42, 96].

Differential impact of behavioral state on hippocampal activity in AD

A recent paper investigated how hippocampal oscillatory activity was affected at late stages of AD during REM sleep, NREM sleep and during awake behaviors in APP/PS1 mice. They observed that the impact of Aβ aggregates on hippocampal neural activity was different between NREM sleep and during wake and REM sleep as hyperactivity was observed during NREM sleep, while hypoactivity was observed during REM sleep and wake [100]. Similarly, a study in the J20 model of AD observed that neuronal hyperexcitability was more prominent in REM sleep, compared to REM sleep [11]. In accordance with these findings, we have observed that hippocampal oscillatory activity during explorative behavior and quiet wakefulness was differentially impacted in TgF344-AD rats during the pre-plaque stage, where we observed decreased theta, fast gamma during quiet wakefulness, but not during exploration [85]. This phenomenon can explain the seemingly contradictory results where we do not observe power alterations during sleep, while we did observe changed oscillatory power during quiet wakefulness in the same cohort of rats [28, 85]. Furthermore, this could in part explain the contradictory findings in SWR duration observed in the current study [85]. Moreover, the current results demonstrate that REM sleep was more severely impacted than NREM sleep further confirming this differential impact of AD pathology on hippocampal activity during different behavioral states.

Theta-gamma coupling in AD

The current study observed a significantly decreased theta- fast gamma coupling in TgF344-AD rats both at the pre- and early-plaque stage of AD. These results are in line with previous electrophysiological studies in TgF344-AD rats, which also observed decreased coupling strengths [77, 78]. Similar decreases were also observed in a variety of mouse models of AD, even before Aβ plaques were present in the brain [27, 54, 64, 75, 76] and in 9 to 12 month old TgF344-AD rats [2, 38, 77, 78], in agreement to the observations in the current study.

In addition, we observed an increased theta slow gamma coupling at the pre-plaque stage, which was restored to WT levels at the early-plaque stage. Bazzigaluppi et al. 2018 observed that PAC between theta and slow gamma was preserved in 6-month-old TgF344-AD rats, similar to the observations in the current study where the coupling between gamma and slow theta is unaltered [2]. Limited information is known about the function of this coupling during REM sleep. However, an electrophysiological study in a mouse model of impaired spatial memory observed an increased coupling strength between theta and slow gamma. Moreover, their results implied that theta-slow gamma coupling reflects a compensatory mechanism to maintain working memory performance. The majority of studies in TgF344-AD rats did not observe working memory deficits in aged rats [69, 83]. Hence, the observed increased slow gamma coupling in the current study in TgF344-AD rats at the pre-plaque stage, might be contributing to the absence of working memory dysfunction in the rats at this age. Future studies correlating working memory dysfunction to theta-gamma coupling could provide valuable insights regarding the electrophysiological underpinnings of working memory dysfunction at early stages of AD.

Compensatory mechanisms at the early-plaque stage in AD

In the current study we observed robust alterations in REM sleep oscillatory activity during REM sleep. The genotypic differences observed at the pre-plaque stage

were larger than the differences at the early-plaque stage, suggesting that oscillatory activity in TgF344-AD rats was partially restored. Interestingly, we observed an increase in cholinergic synapses in the hippocampal regions of TgF344-AD rats, a mechanism postulated to be a sign of compensation for loss of cholinergic tone at earlier stages [25, 36, 49]. Similar increases in cholinergic synapses have been observed at pre-plaque stages in APP/PS1 mice and MCI patients [23, 36].

The REM-associated alterations in hippocampal oscillations in this study are strongly modulated by the cholinergic system [10, 34, 92], strengthening the assumption that compensatory mechanisms are present at 6 months of age in TgF344-AD rats. Similar to the observations in the current study, research has demonstrated that alterations in theta-gamma coupling could be recovered by administration of cholinesterase inhibitors in aged APP/PS1 mice [100]. In addition, donepezil, a commonly used acetylcholinesterase inhibitor, restored decreased theta-fast gamma coupling in aged TgF344-AD rats [77]. These results suggest that the observed increase in cholinergic synapses might be an important endogenous mechanism to slow down disease progression in AD, by restoring the network imbalance [7, 36]. A recent study observed early hyperactivity of cholinergic neurons in different mouse models of AD, supporting our findings of the increased cholinergic synapses. This study also demonstrated that the observed cholinergic hyperactivity contributed to the epileptiform hippocampal activity, which is in contrast to the partial restoration of hippocampal oscillatory activity that we observed. However, the increased activity of the cholinergic system at early stages of AD might be contributing to the vulnerability of this system [31]. Hence, counteracting the early increase in cholinergic activity might be beneficial to prevent the degeneration of cholinergic neurons observed in late AD [51]. This could be an interesting target for future studies.

Limitations of the study

This study only included male rats, to limit sample size, as including females would require a larger number of animals. AD pathology is known to have sex-specific effects, as in women, AD prevalence is higher, and AD progression is faster. In TgF344-AD rats, male rats are more severely affected, as amyloidosis, synaptic dysfunction and cognitive deficits occur earlier in male rats, compared to females [71, 73]. For example, synaptic dysfunction in the perforant pathway was observed in 6-month old male rats, whereas this was only observed in 9-month old female rats [73]. Moreover, within the females, changes in hormone levels due to the estrus cycle are known to interfere with hippocampal synaptic plasticity, hence could induce more variability in our dataset. Many studies used ovariectomized female rats to perform their electrophysiological recordings on, in order to avoid this modulation of synaptic plasticity by estrous cycle changes [33, 74]. However, given the importance of including both males and females to improve translation of the current findings, we suggest that future studies should include males and females, to examine if the sleep disturbances observed in the current study are generalizable across sexes. Another limitation of the current study is the low sample size, which may lead to reduced statistical power, and which can compromise generalizability of the findings. The lack of significant genotypical differences in sleep macro-architecture might be a result of this low sample size. Post-hoc power analyses using the effect sizes obtained from the current study demonstrated that, to find genotypical differences in sleep macro-architecture, more specifically the amount of time spent in REM sleep, we would need almost 60 animals. Regarding the sleep micro-architecture, we mainly observed robust differences in the PAC and SWR parameters, but not in oscillatory power. Power analysis using the obtained effect sizes on fast gamma power during REM and HFO power during NREM demonstrated that we would need at least 42 or 55 subjects to observe genotypical differences in these parameters. These results indeed suggest that the current study mainly observed very strong AD-related differences, but might have missed more subtle differences due to a lack of power. Future studies including more subjects are recommended to confirm the current findings. Moreover, evaluation of sleep micro-, and macroarchitecture at later stages of the disease, would be valuable.

It would be interesting to assess changes in oscillatory behavior between different molecular layers within the CA1 region, to gain more insight into the alterations synaptic transmission, as different layers within CA1 have different in and outputs. In the current manuscript, we did not include this layer-specific analyses, due to the spacing of the electrode sites in our electrodes, which did not allow these types of analyses. Future studies using more densely spaced electrodes evaluating alterations in hippocampal activity within CA1 could be valuable.

A fourth limitation is that the synaptic stainings were performed in a separate cohort, limiting the direct correlation between the number of cholinergic synapses and hippocampal oscillatory activity.

Conclusion

The results from the current study demonstrated subtle micro-architectural changes during NREM sleep, where the duration of SWRs was increased. Disruption of hippocampal activity during REM sleep (e.g. increased theta-slow gamma coupling and decreased theta- fast gamma coupling) were observed at the pre-plaque stage, thus in the absence of Aβ plaques. Moreover, hippocampal

theta-gamma coupling was partially normalized during the early-plaque stage. This recovery coincided with an increased number of cholinergic synapses in the hippocampus, suggesting a role of cholinergic signaling in the restoration of hippocampal activity during the early-plaque stage of AD. The changes in hippocampal activity during sleep preceded robust changes in sleep macroarchitecture, where besides a hint towards REM sleep fragmentation at the pre-plaque stage, time spent in different sleep states and NREM bout length was not different in TgF344-AD rats. Future studies evaluating the presence of early changes in sleep micro-architecture in other AD models or patients at risk of developing AD might lead to novel strategies in order to detect AD at early, presymptomatic stages.

Abbreviations

AD	Alzheimer's Disease
Aβ	Amyloid-beta
ANOVA	analysis of variance
AP	Anterior-posterior
CA	Cornu Ammonis
DG	Dentate Gyrus
DV	Dorsal ventral
EMG	Electromyography
E/I	Excitatory/inhibitory
FDR	False discovery rate
Hz	Hertz
LFP	Local field potentials
LC	Locus Coeruleus
ML	Medial-lateral
mm	millimeter
MI	Modulation index
NREM	Non rapid eye movement
PFA	Paraformaldehyde
PSF	Peak spectral frequency
PAC	Phase-amplitude coupling
Pyr	pyramidal layer
REM	Rapid eye movement
SW	Sharp wave
SWR	Sharp wave-ripples
Tg	TgF344-AD
tPAC	time resolved phase-amplitude coupling
WT	Wildtype
Z	Zeitgeber

Supplementary Information

The online version contains supplementary material available at https://doi.org/10.1186/s40478-025-02016-w.

Supplementary Material 1

Acknowledgements

We are grateful to Karen Sterck, Sofie Thys, Zoë Embrechts and Elien Theuns of the laboratory of Cell Biology & Histology for their support with the immunohistochemical studies.

Author contributions

Monica van den Berg: conceptualization - data curation - formal analysis – investigation – methodology - project administration – software – visualization – writing (original draft). Loran Heymans: Validation - formal analysis - writing (review & editing). Daniëlle Toen: formal analysis – investigation - writing (review & editing). Mohit Adhikari: formal analysis – software - writing (review & editing). Johan van Audekerke: Resources - writing (review & editing). Marlies Verschuuren: methodology – software - writing (review & editing). Isabel Pintelon: investigation – methodology - project administration - writing (review & editing). Winnok H. De Vos: conceptualization - supervision – writing (review & editing). Marleen Verhoye: conceptualization - data curation – funding acquisition - supervision – writing (original draft), writing (review & editing). Georgios A. Keliris: conceptualization – investigation – methodology – formal analysis - funding acquisition - validation - supervision – writing (original draft), writing (review & editing).

Funding

This study was supported by the Fund of Scientific Research Flanders (FWO-G048917N, FWO-G045420N) and the Stichting Alzheimer Onderzoek (SAO-FRA-20180003). The computational resources and services used in this work were provided by the HPC core facility CalcUA of the University of Antwerp, the VSC (Flemish Supercomputer Center), funded by the Hercules Foundation and the Flemish Government department EWI. M Verschuren, WDV and IP are supported by the Research Foundation Flanders FWO (I000321N, I003420N).

Data availability

The electrophysiological datasets generated during the current study are publicly available in the OpenNeuro repository (ds004651).

Declarations

Ethics approval and consent to participate

All procedures were in accordance with the guidelines approved by the European Ethics Committee (decree 2010/63/EU) and were approved by the Committee on Animal Care and Use at the University of Antwerp, Belgium (approval number: 2019-06).

Consent for publication

Not applicable.

Competing interests

The authors declare that they have no competing interests.

Author details

[1]Bio-Imaging Lab, University of Antwerp, Campus Drie Eiken – Building UC, Universiteitsplein 1, Wilrijk 2610, Belgium
[2]Laboratory of Cell Biology and Histology, University of Antwerp, Universiteitsplein 1, Wilrijk 2610, Belgium
[3]Antwerp Centre for Advanced Microscopy, Universiteitsplein 1, Antwerp, Wilrijk 2610, Belgium
[4]Department of Neurology - Brigham and Women's Hospital, Harvard Medical School, Boston, USA
[5]μNEURO Research Centre of Excellence, University of Antwerp, Antwerp, Belgium

Received: 1 July 2024 / Accepted: 23 April 2025
Published online: 10 May 2025

References

1. Alger BE, Nagode DA, Tang AH (2014) Muscarinic cholinergic receptors modulate inhibitory synaptic rhythms in hippocampus and neocortex. Front Synaptic Neurosci 6:18. https://doi.org/10.3389/fnsyn.2014.00018
2. Bazzigaluppi P, Beckett TL, Koletar MM, Lai AY, Joo IL, Brown ME, Carlen PL, McLaurin J, Stefanovic B (2018) Early-stage Attenuation of phase-amplitude coupling in the hippocampus and medial prefrontal cortex in a Transgenic rat model of Alzheimer's disease. J Neurochem 144:669–679. https://doi.org/10.1111/jnc.14136
3. Belluscio MA, Mizuseki K, Schmidt R, Kempter R, Buzsaki G (2012) Cross-frequency phase-phase coupling between theta and gamma oscillations in the hippocampus. J Neurosci 32:423–435. https://doi.org/10.1523/JNEUROSCI.4122-11.2012
4. Benthem SD, Skelin I, Moseley SC, Stimmell AC, Dixon JR, Melilli AS, Molina L, McNaughton BL, Wilber AA (2020) Impaired Hippocampal-Cortical Interactions during Sleep in a Mouse Model of Alzheimer's Disease. Curr Biol 30:2588–2601 e2585 https://doi.org/10.1016/j.cub.2020.04.087

5. Bergmann TO, Born J (2018) Phase-Amplitude coupling: A general mechanism for memory processing and synaptic plasticity?? Neuron 97:10–13. https://doi.org/10.1016/j.neuron.2017.12.023
6. Bieri KW, Bobbitt KN, Colgin LL (2014) Slow and fast gamma rhythms coordinate different Spatial coding modes in hippocampal place cells. Neuron 82:670–681. https://doi.org/10.1016/j.neuron.2014.03.013
7. Bott JB, Heraud C, Cosquer B, Herbeaux K, Aubert J, Sartori M, Goutagny R, Mathis C (2016) APOE-Sensitive cholinergic sprouting compensates for hippocampal dysfunctions due to reduced entorhinal input. J Neurosci 36:10472–10486. https://doi.org/10.1523/JNEUROSCI.1174-16.2016
8. Braak H, Braak E (1991) Neuropathological stageing of Alzheimer-related changes. Acta Neuropathol 82:239–259. https://doi.org/10.1007/BF00308809
9. Braak H, Thal DR, Ghebremedhin E, Del Tredici K (2011) Stages of the pathologic process in alzheimer disease: age categories from 1 to 100 years. J Neuropathol Exp Neurol 70:960–969. https://doi.org/10.1097/NEN.0b013e318232a379
10. Brown RE, Basheer R, McKenna JT, Strecker RE, McCarley RW (2012) Control of sleep and wakefulness. Physiol Rev 92:1087–1187. https://doi.org/10.1152/physrev.00032.2011
11. Brown R, Lam AD, Gonzalez-Sulser A, Ying A, Jones M, Chou RC, Tzioras M, Jordan CY, Jedrasiak-Cape I, Hemonnot AL et al (2018) Circadian and Brain State Modulation of Network Hyperexcitability in Alzheimer's Disease. eNeuro 5: https://doi.org/10.1523/ENEURO.0426-17.2018
12. Buzsaki G (2015) Hippocampal Sharp wave-ripple: A cognitive biomarker for episodic memory and planning. Hippocampus 25:1073–1188. https://doi.org/10.1002/hipo.22488
13. Buzsaki G, Buhl DL, Harris KD, Csicsvari J, Czeh B, Morozov A (2003) Hippocampal network patterns of activity in the mouse. Neuroscience 116:201–211. https://doi.org/10.1016/s0306-4522(02)00669-3
14. Byron N, Semenova A, Sakata S (2021) Mutual Interactions between Brain States and Alzheimer's Disease Pathology: A Focus on Gamma and Slow Oscillations. Biology (Basel) 10. https://doi.org/10.3390/biology10080707
15. Caccavano A, Bozzelli PL, Forcelli PA, Pak DTS, Wu JY, Conant K, Vicini S (2020) Inhibitory parvalbumin basket cell activity is selectively reduced during hippocampal Sharp wave ripples in a mouse model of Familial Alzheimer's disease. J Neurosci 40:5116–5136. https://doi.org/10.1523/JNEUROSCI.0425-20.2020
16. Canolty RT, Edwards E, Dalal SS, Soltani M, Nagarajan SS, Kirsch HE, Berger MS, Barbaro NM, Knight RT (2006) High gamma power is phase-locked to theta oscillations in human neocortex. Science 313:1626–1628. https://doi.org/10.1126/science.1128115
17. Casagrande M, Forte G, Favieri F, Corbo I (2022) Sleep Quality and Aging: A Systematic Review on Healthy Older People, Mild Cognitive Impairment and Alzheimer's Disease. Int J Environ Res Public Health 19. https://doi.org/10.3390/ijerph19148457
18. Castano-Prat P, Perez-Mendez L, Perez-Zabalza M, Sanfeliu C, Gimenez-Llort L, Sanchez-Vives MV (2019) Altered slow (< 1 Hz) and fast (beta and gamma) neocortical oscillations in the 3xTg-AD mouse model of Alzheimer's disease under anesthesia. Neurobiol Aging 79:142–151. https://doi.org/10.1016/j.neurobiolaging.2019.02.009
19. Cirrito JR, Yamada KA, Finn MB, Sloviter RS, Bales KR, May PC, Schoepp DD, Paul SM, Mennerick S, Holtzman DM (2005) Synaptic activity regulates interstitial fluid amyloid-beta levels in vivo. Neuron 48:913–922. https://doi.org/10.1016/j.neuron.2005.10.028
20. Cohen RM, Rezai-Zadeh K, Weitz TM, Rentsendorj A, Gate D, Spivak I, Bholat Y, Vasilevko V, Glabe CG, Breunig JJ al (2013) A Transgenic alzheimer rat with plaques, Tau pathology, behavioral impairment, oligomeric Abeta, and Frank neuronal loss. J Neurosci 33:6245–6256. https://doi.org/10.1523/JNEUROSCI.3672-12.2013
21. Colgin LL (2015) Theta-gamma coupling in the entorhinal-hippocampal system. Curr Opin Neurobiol 31:45–50. https://doi.org/10.1016/j.conb.2014.08.001
22. Colgin LL (2016) Rhythms of the hippocampal network. Nat Rev Neurosci 17:239–249. https://doi.org/10.1038/nrn.2016.21
23. DeKosky ST, Ikonomovic MD, Styren SD, Beckett L, Wisniewski S, Bennett DA, Cochran EJ, Kordower JH, Mufson EJ (2002) Upregulation of choline acetyltransferase activity in hippocampus and frontal cortex of elderly subjects with mild cognitive impairment. Ann Neurol 51:145–155. https://doi.org/10.1002/ana.10069
24. Diekelmann S, Born J (2010) The memory function of sleep. Nat Rev Neurosci 11:114–126. https://doi.org/10.1038/nrn2762
25. Dubelaar EJ, Mufson EJ, ter Meulen WG, Van Heerikhuize JJ, Verwer RW, Swaab DF (2006) Increased metabolic activity in nucleus basalis of meynert neurons in elderly individuals with mild cognitive impairment as indicated by the size of the golgi apparatus. J Neuropathol Exp Neurol 65:257–266. https://doi.org/10.1097/01.jnen.0000205143.16339.cd
26. Ego-Stengel V, Wilson MA (2010) Disruption of ripple-associated hippocampal activity during rest impairs Spatial learning in the rat. Hippocampus 20:1–10. https://doi.org/10.1002/hipo.20707
27. Etter G, van der Veldt S, Manseau F, Zarrinkoub I, Trillaud-Doppia E, Williams S (2019) Optogenetic gamma stimulation rescues memory impairments in an Alzheimer's disease mouse model. Nat Commun 10:5322. https://doi.org/10.1038/s41467-019-13260-9
28. Faraz Moradi MB, Mirjebreili M, Kosten L, Verhoye M, Amiri M, Keliris GA (2022) Early Electrophysiological Aberrations in the Hippocampus of the TgF344-AD Rat Model as a Potential Biomarker for Alzheimer's Disease Prognosis. BioRxiv: https://doi.org/10.1101/2022.07.01.498373
29. Fernandez-Ruiz A, Oliva A, Fermino de Oliveira E, Rocha-Almeida F, Tingley D, Buzsaki G (2019) Long-duration hippocampal Sharp wave ripples improve memory. Science 364:1082–1086. https://doi.org/10.1126/science.aax0758
30. Geschwill P, Kaiser ME, Grube P, Lehmann N, Thome C, Draguhn A, Hollnagel JO, Both M (2020) Synchronicity of excitatory inputs drives hippocampal networks to distinct oscillatory patterns. Hippocampus 30:1044–1057. https://doi.org/10.1002/hipo.23214
31. Geula C, Dunlop SR, Ayala I, Kawles AS, Flanagan ME, Gefen T, Mesulam MM (2021) Basal forebrain cholinergic system in the dementias: vulnerability, resilience, and resistance. J Neurochem 158:1394–1411. https://doi.org/10.1111/jnc.15471
32. Goodman MS, Kumar S, Zomorrodi R, Ghazala Z, Cheam ASM, Barr MS, Daskalakis ZJ, Blumberger DM, Fischer C, Flint A et al (2018) Theta-Gamma Coupling and Working Memory in Alzheimer's Dementia and Mild Cognitive Impairment. Front Aging Neurosci 10: 101 https://doi.org/10.3389/fnagi.2018.00101
33. Goodman AM, Langner BM, Jackson N, Alex C, McMahon LL (2021) Heightened hippocampal beta-Adrenergic receptor function drives synaptic potentiation and supports learning and memory in the TgF344-AD rat model during prodromal Alzheimer's disease. J Neurosci 41:5747–5761. https://doi.org/10.1523/JNEUROSCI.0119-21.2021
34. Gu Z, Yakel JL (2022) Cholinergic regulation of hippocampal Theta rhythm. Biomedicines 10. https://doi.org/10.3390/biomedicines10040745
35. Holth JK, Mahan TE, Robinson GO, Rocha A, Holtzman DM (2017) Altered sleep and EEG power in the P301S Tau Transgenic mouse model. Ann Clin Transl Neurol 4:180–190. https://doi.org/10.1002/acn3.390
36. Hu L, Wong TP, Cote SL, Bell KF, Cuello AC (2003) The impact of Abeta-plaques on cortical cholinergic and non-cholinergic presynaptic boutons in Alzheimer's disease-like Transgenic mice. Neuroscience 121:421–432. https://doi.org/10.1016/s0306-4522(03)00394-4
37. Igarashi KM, Lu L, Colgin LL, Moser MB, Moser EI (2014) Coordination of entorhinal-hippocampal ensemble activity during associative learning. Nature 510:143–147. https://doi.org/10.1038/nature13162
38. Joo IL, Lai AY, Bazzigaluppi P, Koletar MM, Dorr A, Brown ME, Thomason LA, Sled JG, McLaurin J, Stefanovic B (2017) Early neurovascular dysfunction in a Transgenic rat model of Alzheimer's disease. Sci Rep 7:46427. https://doi.org/10.1038/srep46427
39. Ju YE, McLeland JS, Toedebusch CD, Xiong C, Fagan AM, Duntley SP, Morris JC, Holtzman DM (2013) Sleep quality and preclinical alzheimer disease. JAMA Neurol 70:587–593. https://doi.org/10.1001/jamaneurol.2013.2334
40. Ju YE, Lucey BP, Holtzman DM (2014) Sleep and alzheimer disease pathology–a bidirectional relationship. Nat Rev Neurol 10:115–119. https://doi.org/10.1038/nrneurol.2013.269
41. Ju YS, Ooms SJ, Sutphen C, Macauley SL, Zangrilli MA, Jerome G, Fagan AM, Mignot E, Zempel JM, Claassen Jet al et al (2017) Slow wave sleep disruption increases cerebrospinal fluid amyloid-beta levels. Brain 140:2104–2111. https://doi.org/10.1093/brain/awx148
42. Jura B, Macrez N, Meyrand P, Bem T (2019) Deficit in hippocampal ripples does not preclude Spatial memory formation in APP/PS1 mice. Sci Rep 9:20129. https://doi.org/10.1038/s41598-019-56582-w
43. Kam K, Duffy AM, Moretto J, LaFrancois JJ, Scharfman HE (2016) Interictal spikes during sleep are an early defect in the Tg2576 mouse model of beta-amyloid neuropathology. Sci Rep 6:20119. https://doi.org/10.1038/srep20119
44. Katsuki F, Gerashchenko D, Brown RE (2022) Alterations of sleep oscillations in Alzheimer's disease: A potential role for GABAergic neurons in the cortex,

hippocampus, and thalamus. Brain Res Bull 187:181–198. https://doi.org/10.1016/j.brainresbull.2022.07.002
45. Kent BA, Strittmatter SM, Nygaard HB (2018) Sleep and EEG power spectral analysis in three Transgenic mouse models of Alzheimer's disease: APP/PS1, 3xTgAD, and Tg2576. J Alzheimers Dis 64:1325–1336. https://doi.org/10.3233/JAD-180260
46. Kent BA, Michalik M, Marchant EG, Yau KW, Feldman HH, Mistlberger RE, Nygaard HB (2019) Delayed daily activity and reduced NREM slow-wave power in the APPswe/PS1dE9 mouse model of Alzheimer's disease. Neurobiol Aging 78:74–86. https://doi.org/10.1016/j.neurobiolaging.2019.01.010
47. Killgore WD (2010) Effects of sleep deprivation on cognition. Prog Brain Res 185:105–129 Doi 10.1016/B978-0-444-53702-7.00007– 5
48. Kincheski GC, Valentim IS, Clarke JR, Cozachenco D, Castelo-Branco MTL, Ramos-Lobo AM, Rumjanek V, Donato J Jr., De Felice FG, Ferreira ST (2017) Chronic sleep restriction promotes brain inflammation and synapse loss, and potentiates memory impairment induced by amyloid-beta oligomers in mice. Brain Behav Immun 64:140–151. https://doi.org/10.1016/j.bbi.2017.04.007
49. Lau P, Bossers K, Janky R, Salta E, Frigerio CS, Barbash S, Rothman R, Sierksma AS, Thathiah A, Greenberg Det al et al (2013) Alteration of the MicroRNA network during the progression of Alzheimer's disease. EMBO Mol Med 5:1613–1634. https://doi.org/10.1002/emmm.201201974
50. Liguori C, Placidi F, Izzi F, Spanetta M, Mercuri NB, Di Pucchio A (2020) Sleep dysregulation, memory impairment, and CSF biomarkers during different levels of neurocognitive functioning in Alzheimer's disease course. Alzheimers Res Ther 12:5. https://doi.org/10.1186/s13195-019-0571-3
51. Lisgaras CP, Scharfman HE (2023) Interictal spikes in Alzheimer's disease: preclinical evidence for dominance of the dentate gyrus and cholinergic control by the medial septum. Neurobiol Dis 187:106294. https://doi.org/10.1016/j.nbd.2023.106294
52. Lucey BP, Bateman RJ (2014) Amyloid-beta diurnal pattern: possible role of sleep in Alzheimer's disease pathogenesis. Neurobiol Aging 35(Suppl 2):S29–34. https://doi.org/10.1016/j.neurobiolaging.2014.03.035
53. Ma T, Klann E (2012) Amyloid beta: linking synaptic plasticity failure to memory disruption in Alzheimer's disease. J Neurochem 120 Suppl 1:140–148. https://doi.org/10.1111/j.1471-4159.2011.07506.x
54. Mably AJ, Gereke BJ, Jones DT, Colgin LL (2017) Impairments in Spatial representations and rhythmic coordination of place cells in the 3xTg mouse model of Alzheimer's disease. Hippocampus 27:378–392. https://doi.org/10.1002/hipo.22697
55. Mander BA, Winer JR, Walker MP (2017) Sleep Hum Aging Neuron 94:19–36. https://doi.org/10.1016/j.neuron.2017.02.004
56. Moguilner SG, Berezuk C, Bender AC, Pellerin KR, Gomperts SN, Cash SS, Sarkis RA, Lam AD (2024) Sleep functional connectivity, hyperexcitability, and cognition in Alzheimer's disease. Alzheimers Dement: https://doi.org/10.1002/alz.13861
57. Molle M, Yeshenko O, Marshall L, Sara SJ, Born J (2006) Hippocampal Sharp wave-ripples linked to slow oscillations in rat slow-wave sleep. J Neurophysiol 96:62–70. https://doi.org/10.1152/jn.00014.2006
58. Moradi F, van den Berg M, Mirjebreili M, Kosten L, Verhoye M, Amiri M, Keliris GA (2022) Early electrophysiological aberrations in the Hippocampus of the TgF344-AD rat model as a potential biomarker for Alzheimer's disease prognosis. BioRxiv: 2022.2007.2001.498373. https://doi.org/10.1101/2022.07.01.498373
59. Mormann F, Fell J, Axmacher N, Weber B, Lehnertz K, Elger CE, Fernandez G (2005) Phase/amplitude reset and theta-gamma interaction in the human medial Temporal lobe during a continuous word recognition memory task. Hippocampus 15:890–900. https://doi.org/10.1002/hipo.20117
60. Newman EL, Gillet SN, Climer JR, Hasselmo ME (2013) Cholinergic Blockade reduces theta-gamma phase amplitude coupling and speed modulation of theta frequency consistent with behavioral effects on encoding. J Neurosci 33:19635–19646. https://doi.org/10.1523/JNEUROSCI.2586-13.2013
61. Oliva A, Fernandez-Ruiz A, Fermino de Oliveira E, Buzsaki G (2018) Origin of Gamma Frequency Power during Hippocampal Sharp-Wave Ripples. Cell Rep 25: 1693–1700 e1694 https://doi.org/10.1016/j.celrep.2018.10.066
62. Oostenveld R, Fries P, Maris E, Schoffelen JM (2011) FieldTrip: open source software for advanced analysis of MEG, EEG, and invasive electrophysiological data. Comput Intell Neurosci 2011:156869. https://doi.org/10.1155/2011/156869
63. Ozcan GG, Lim S, Leighton P, Allison WT, Rihel J (2020) Sleep is bi-directionally modified by amyloid beta oligomers. Elife 9. https://doi.org/10.7554/eLife.53995
64. Park K, Lee J, Jang HJ, Richards BA, Kohl MM, Kwag J (2020) Optogenetic activation of parvalbumin and somatostatin interneurons selectively restores theta-nested gamma oscillations and oscillation-induced Spike timing-dependent long-term potentiation impaired by amyloid beta oligomers. BMC Biol 18:7. https://doi.org/10.1186/s12915-019-0732-7
65. Proskauer Pena SL, Mallouppas K, Oliveira AMG, Zitricky F, Nataraj A, Jezek K (2021) Early Spatial Memory Impairment in a Double Transgenic Model of Alzheimer's Disease TgF-344 AD. Brain Sci 11. https://doi.org/10.3390/brainsci11101300
66. Ratner MH, Downing SS, Guo O, Odamah KE, Stewart TM, Kumaresan V, Robitsek RJ, Xia W, Farb DH (2021) Prodromal dysfunction of alpha5GABA-A receptor modulated hippocampal ripples occurs prior to neurodegeneration in the TgF344-AD rat model of Alzheimer's disease. Heliyon 7:e07895. https://doi.org/10.1016/j.heliyon.2021.e07895
67. Roh JH, Huang Y, Bero AW, Kasten T, Stewart FR, Bateman RJ, Holtzman DM (2012) Disruption of the sleep-wake cycle and diurnal fluctuation of beta-amyloid in mice with Alzheimer's disease pathology. Sci Transl Med 4:150ra122. https://doi.org/10.1126/scitranslmed.3004291
68. Rosinvil T, Bouvier J, Dube J, Lafreniere A, Bouchard M, Cyr-Cronier J, Gosselin N, Carrier J, Lina JM (2021) Are age and sex effects on sleep slow waves only a matter of electroencephalogram amplitude? Sleep 44. https://doi.org/10.1093/sleep/zsaa186
69. Sagalajev B, Lennartz L, Vieth L, Gunawan CT, Neumaier B, Drzezga A, Visser-Vandewalle V, Endepols H, Sesia T (2023) TgF344-AD rat model of Alzheimer's disease: Spatial disorientation and asymmetry in hemispheric neurodegeneration. J Alzheimers Dis Rep 7:1085–1094. https://doi.org/10.3233/ADR-230038
70. Sanchez-Aguilera A, Quintanilla JP (2021) Sharp wave ripples in Alzheimer's disease: in search of mechanisms. J Neurosci 41:1366–1370. https://doi.org/10.1523/JNEUROSCI.2020-20.2020
71. Sare RM, Cooke SK, Krych L, Zerfas PM, Cohen RM, Smith CB (2020) Behavioral phenotype in the TgF344-AD rat model of Alzheimer's disease. Front Neurosci 14:601. https://doi.org/10.3389/fnins.2020.00601
72. Schindelin J, Arganda-Carreras I, Frise E, Kaynig V, Longair M, Pietzsch T, Preibisch S, Rueden C, Saalfeld S, Schmid Bet al et al (2012) Fiji: an open-source platform for biological-image analysis. Nat Methods 9:676–682. https://doi.org/10.1038/nmeth.2019
73. Smith LA, McMahon LL (2018) Deficits in synaptic function occur at medial perforant path-dentate granule cell synapses prior to Schaffer collateral-CA1 pyramidal cell synapses in the novel TgF344-Alzheimer's disease rat model. Neurobiol Dis 110:166–179. https://doi.org/10.1016/j.nbd.2017.11.014
74. Smith LA, Goodman AM, McMahon LL (2022) Dentate granule cells are hyperexcitable in the TgF344-AD rat model of Alzheimer's disease. Front Synaptic Neurosci 14:826601. https://doi.org/10.3389/fnsyn.2022.826601
75. Stoiljkovic M, Kelley C, Nagy D, Hajos M (2015) Modulation of hippocampal neuronal network oscillations by alpha7 nACh receptors. Biochem Pharmacol 97:445–453. https://doi.org/10.1016/j.bcp.2015.06.031
76. Stoiljkovic M, Kelley C, Hajos GP, Nagy D, Koenig G, Leventhal L, Hajos M (2016) Hippocampal network dynamics in response to alpha7 nACh receptors activation in amyloid-beta overproducing Transgenic mice. Neurobiol Aging 45:161–168. https://doi.org/10.1016/j.neurobiolaging.2016.05.021
77. Stoiljkovic M, Kelley C, Horvath TL, Hajos M (2018) Neurophysiological signals as predictive translational biomarkers for Alzheimer's disease treatment: effects of donepezil on neuronal network oscillations in TgF344-AD rats. Alzheimers Res Ther 10:105. https://doi.org/10.1186/s13195-018-0433-4
78. Stoiljkovic M, Kelley C, Stutz B, Horvath TL, Hajos M (2019) Altered cortical and hippocampal excitability in TgF344-AD rats modeling Alzheimer's disease pathology. Cereb Cortex 29:2716–2727. https://doi.org/10.1093/cercor/bhy140
79. Tadel F, Baillet S, Mosher JC, Pantazis D, Leahy RM (2011) Brainstorm: a user-friendly application for MEG/EEG analysis. Comput Intell Neurosci 2011:879716. https://doi.org/10.1155/2011/879716
80. Tamura M, Spellman TJ, Rosen AM, Gogos JA, Gordon JA (2017) Hippocampal-prefrontal theta-gamma coupling during performance of a Spatial working memory task. Nat Commun 8:2182. https://doi.org/10.1038/s41467-017-02108-9
81. Tort AB, Komorowski RW, Manns JR, Kopell NJ, Eichenbaum H (2009) Theta-gamma coupling increases during the learning of item-context associations. Proc Natl Acad Sci U S A 106:20942–20947. https://doi.org/10.1073/pnas.0911331106

82. Tort AB, Komorowski R, Eichenbaum H, Kopell N (2010) Measuring phase-amplitude coupling between neuronal oscillations of different frequencies. J Neurophysiol 104:1195–1210. https://doi.org/10.1152/jn.00106.2010
83. Tournier BB, Barca C, Fall AB, Gloria Y, Meyer L, Ceyzeriat K, Millet P (2021) Spatial reference learning deficits in absence of dysfunctional working memory in the TgF344-AD rat model of Alzheimer's disease. Genes Brain Behav 20:e12712. https://doi.org/10.1111/gbb.12712
84. van den Berg M, Adhikari MH, Verschuuren M, Pintelon I, Vasilkovska T, Van Audekerke J, Missault S, Heymans L, Ponsaerts P, De Vos WH et al (2022) Altered basal forebrain function during whole-brain network activity at pre- and early-plaque stages of Alzheimer's disease in TgF344-AD rats. Alzheimers Res Ther 14: 148 https://doi.org/10.1186/s13195-022-01089-2
85. van den Berg M, Toen D, Verhoye M, Keliris GA (2023) Alterations in theta-gamma coupling and Sharp wave-ripple, signs of prodromal hippocampal network impairment in the TgF344-AD rat model. Front Aging Neurosci 15:1081058. https://doi.org/10.3389/fnagi.2023.1081058
86. Van Egroo M, Koshmanova E, Vandewalle G, Jacobs HIL (2022) Importance of the locus coeruleus-norepinephrine system in sleep-wake regulation: implications for aging and Alzheimer's disease. Sleep Med Rev 62:101592. https://doi.org/10.1016/j.smrv.2022.101592
87. Van Erum J, Van Dam D, De Deyn PP (2019) Alzheimer's disease: neurotransmitters of the sleep-wake cycle. Neurosci Biobehav Rev 105:72–80. https://doi.org/10.1016/j.neubiorev.2019.07.019
88. Vazquez J, Baghdoyan HA (2001) Basal forebrain acetylcholine release during REM sleep is significantly greater than during waking. Am J Physiol Regul Integr Comp Physiol 280:R598–601. https://doi.org/10.1152/ajpregu.2001.280.2.R598
89. Verschuuren M, Verstraelen P, Garcia-Diaz Barriga G, Cilissen I, Coninx E, Verslegers M, Larsen PH, Nuydens R, De Vos WH (2019) High-throughput microscopy exposes a Pharmacological window in which dual leucine zipper kinase Inhibition preserves neuronal network connectivity. Acta Neuropathol Commun 7:93. https://doi.org/10.1186/s40478-019-0741-3
90. Verstraelen P, Garcia-Diaz Barriga G, Verschuuren M, Asselbergh B, Nuydens R, Larsen PH, Timmermans JP, De Vos WH (2020) Systematic quantification of synapses in primary neuronal culture. iScience 23:101542. https://doi.org/10.1016/j.isci.2020.101542
91. Wang J, Ikonen S, Gurevicius K, van Groen T, Tanila H (2002) Alteration of cortical EEG in mice carrying mutated human APP transgene. Brain Res 943:181–190. https://doi.org/10.1016/s0006-8993(02)02617-3
92. Watson CJ, Baghdoyan HA, Lydic R (2012) Neuropharmacology of sleep and wakefulness: 2012 update. Sleep Med Clin 7:469–486. https://doi.org/10.1016/j.jsmc.2012.06.010
93. Witton J, Staniaszek LE, Bartsch U, Randall AD, Jones MW, Brown JT (2016) Disrupted hippocampal sharp-wave ripple-associated Spike dynamics in a Transgenic mouse model of dementia. J Physiol 594:4615–4630. https://doi.org/10.1113/jphysiol.2014.282889
94. Xie L, Kang H, Xu Q, Chen MJ, Liao Y, Thiyagarajan M, O'Donnell J, Christensen DJ, Nicholson C, Iliff JJet al et al (2013) Sleep drives metabolite clearance from the adult brain. Science 342:373–377. https://doi.org/10.1126/science.1241224
95. Xu Y, Zhao M, Han Y, Zhang H (2020) GABAergic inhibitory interneuron deficits in Alzheimer's disease: implications for treatment. Front Neurosci 14:660. https://doi.org/10.3389/fnins.2020.00660
96. Yang H, Jeong Y (2021) Correlation between alteration of Sharp-wave ripple coupled cortical Oscillation and Long-term memory deficit in alzheimer disease model mice. Exp Neurobiol 30:430–440. https://doi.org/10.5607/en21046
97. Zarhin D, Atsmon R, Ruggiero A, Baeloha H, Shoob S, Scharf O, Heim LR, Buchbinder N, Shinikamin O, Shapira Iet al et al (2022) Disrupted neural correlates of anesthesia and sleep reveal early circuit dysfunctions in alzheimer models. Cell Rep 38:110268. https://doi.org/10.1016/j.celrep.2021.110268
98. Zhang F, Zhong R, Li S, Fu Z, Wang R, Wang T, Huang Z, Le W (2019) Alteration in sleep architecture and electroencephalogram as an early sign of Alzheimer's disease preceding the disease pathology and cognitive decline. Alzheimers Dement 15:590–597. https://doi.org/10.1016/j.jalz.2018.12.004
99. Zhen ZH, Guo MR, Li HM, Guo OY, Zhen JL, Fu J, Tan GJ (2021) Normal and abnormal Sharp wave ripples in the Hippocampal-Entorhinal cortex system: implications for memory consolidation, Alzheimer's disease, and Temporal lobe epilepsy. Front Aging Neurosci 13:683483. https://doi.org/10.3389/fnagi.2021.683483
100. Zhou H, Li H, Gowravaram N, Quan M, Kausar N, Gomperts SN (2022) Disruption of hippocampal neuronal circuit function depends upon behavioral state in the APP/PS1 mouse model of Alzheimer's disease. Sci Rep 12:21022. https://doi.org/10.1038/s41598-022-25364-2

Publisher's note